Proceedings of the 9th International Conference on Structural Dynamics, EURODYN 2014
Porto, Portugal, 30 June - 2 July 2014
A. Cunha, E. Caetano, P. Ribeiro, G. Müller (eds.)
ISSN: 2311-9020; ISBN: 978-972-752-165-4

Railway vibration: Predicting the field performances of mitigation measures in buildings

Michel Villot[1], Philippe Jean[1]
[1]Heatlth & Comfort Department, CSTB, R. Joseph Fourier, 38400 Saint Martin d'Hères, France

e-mail: michel.villot@cstb.fr, philippe.jean@cstb.fr

ABSTRACT: Mitigation measures against railway vibration in buildings consist of elastomeric mounts or springs inserted between building foundations and upper-structures. This paper aims at predicting and checking on site the field performances of such mitigation measures expressed as a power flow insertion gain. The predicted performance is estimated from the mobilities of the isolation mounts (given by the manufacturer) and the mobilities of the supporting building structures, obtained either from measurements or from calculation using a ground structure vibration model (CSTB MEFISSTO software). The "on site" performance is estimated from velocity measurements on both sides of the isolator. Both compressional and shear wave transmissions into building are discussed. The approach is numerically validated in the simple case of a 2D building on homogeneous ground excited by any surface activity and its limits are identified.

KEY WORDS: railway vibration; mitigation measures in buildings; power flow insertion gain.

1 INTRODUCTION

Mitigation measures against railway vibration in buildings consist of elastomeric mounts or springs inserted between building foundations and upper-structures. The method for predicting their performances is usually simplistic and based on the dynamic transmissibility of a single degree of freedom mass-spring oscillator. A more realistic way of assessing isolation performance has been proposed in [1], where the performance is expressed as a power flow insertion gain (thus allowing several degrees of freedom), estimated using a 2D "building on pile" model.

The approach discussed below predicts the performance of isolation mounts in terms of a power flow insertion gain estimated from the mobility of the isolation mounts (given by the manufacturer) and the mobilities of the supporting building structures, obtained in this paper from calculation using a ground structure vibration model (CSTB MEFISSTO software). The approach also includes an "on site" checking of the isolator performance. The method is then numerically validated in the simple case of a 2D building on homogeneous ground excited by surface activity (vertical force applied on ground surface).

2 PERFORMANCE PREDICTION

2.1 Performance definition

The mitigation measure consists in inserting an isolator between source (building foundations) and receiver (building upper-structure) as show in Figure 1; the performance can be expressed as in [1] as a Power Flow Insertion Gain (PFIG) in dB defined from the ratio between the vibration power flows transmitted to the receiver with and without the isolator:

$$PFIG = 10.\lg(\Pi_{isol} / \Pi_{unisol}) \quad (1)$$

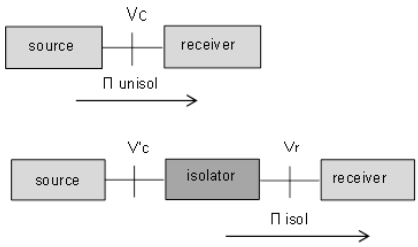

Figure 1. Source-receiver isolated system.

2.2 Performance prediction

Assuming a one degree-of-freedom (dof) source receiver system, source, receiver and isolator can then be characterized by their mobility Y (ratio between velocity response and force applied) as show in Figure 2.

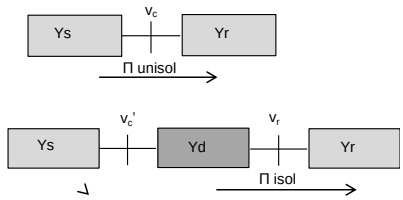

Figure 2. One degree of freedom source-receiver isolated system.

Contact velocity v_c, contact force f_c and power transmitted $\prod_{unisol}$ can be expressed in terms of the source free velocity v_L (source velocity when not connected to the receiver) and the source and receiver mobilities as [2]:

$$f_c = v_L / (Y_S + Y_R) \quad (2)$$

$$v_c = v_L . Y_R / (Y_S + Y_R) \quad (3)$$

$$\Pi_{unisol} = v_{L,rms}^2 . \mathrm{Re}(Y_R) / |Y_S + Y_R|^2 \quad (4)$$

All the quantities in equations (2) and (3) are complex.

The same equations can be written for the isolated system (of mobility $Y_R' = Y_d + Y_R$):

$$f_c' = v_L / (Y_S + Y_R') \quad (5)$$

$$v_c' = v_L . Y_R' / (Y_S + Y_R') \approx v_L \quad (6)$$

since Y_R' is supposed to be large compared to Y_S.

Assuming the mass of the isolator negligible, the contact force f_c' is transmitted to the receiver, leading to:

$$f_c' = v_L / (Y_S + Y_R') = v_r / Y_R \quad (7)$$

which allows calculating $\prod_{isol}$:

$$\Pi_{isol} = \frac{1}{2} \mathrm{Re}(f_c'.v_r^*) = v_{L,rms}^2 . \mathrm{Re}(Y_R) / |Y_S + Y_R'|^2 \quad (8)$$

The PFIG can then be deduced from equations (4) and (8) and estimated as:

$$PFIG = 10.\lg(|Y_S + Y_R|^2 / |Y_S + Y_R + Y_d|^2) \quad (9)$$

This PFIG estimation allows predicting the isolation performance, assuming the mobility of the source, the receiver and the isolator are known.

2.3 *On site performance test*

Assuming again a one dof source receiver system, the PFIG can also be expressed in terms of the isolator upstream and downstream velocities (respectively v_c' and v_r), which can be measured on site, thus allowing checking the isolator performance on site.

The powers $\prod_{isol}$ and $\prod_{unisol}$ can be written as:

$$\Pi_{isol} = v_{r,rms}^2 . \mathrm{Re}(Y_R) / |Y_R|^2 \quad (10)$$

$$\Pi_{unisol} = v_{c,rms}^2 . \mathrm{Re}(Y_R) / |Y_R|^2 \quad (11)$$

which leads to:

$$PFIG = 10.\lg(v_{r,rms}^2 / v_{c,rms}^2) \quad (12)$$

Expressing v_c as a function of v_c' from equations (3) and (6) leads to:

$$PFIG \approx 10.\lg(\frac{v_{r,rms}^2}{v'^2_{c,rms}} .(|Y_R + Y_S|^2 / |Y_R|^2) \quad (13)$$

This PFIG expression allows checking the isolation performance on site from measurements of the isolator upstream and downstream velocities and assuming the mobility of the source and the receiver are known.

2.4 *Multi dof source receiver systems*

In the case of multi dof source-receiver systems involving both longitudinal and bending wave transmissions, similar transmitted powers (as in section 2.2) can be calculated for each dof, (assuming no correlation between dof) and added to obtain the total power; however the resulting PFIG expression becomes much more complicated and difficult to predict, since it not only depends on the mobilities, but also on the source free velocities.

In the case of multi dof source-receiver systems involving several contact points between source and receiver, the total power transmitted at each contact point can be expressed in terms of the source and receiver effective mobilities [4], which can be approximated from the knowledge of both input and transfer mobilities; the powers and the resulting PFIG are therefore more difficult to predict.

3 NUMERICAL VALIDATION

3.1 *Ground building model*

A 2D ground building model has been used for validation; the calculations are fast and 2D configurations are realistic enough, corresponding to cases, where isolation mounts are distributed along walls.

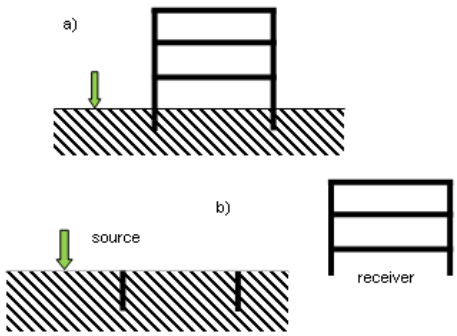

Figure 3. 2D ground building configurations considered

The 2D configurations given in Figure 3 have been used to numerically estimate the following quantities:

- the ground-building configuration in Figure 3a allows estimating the building floor velocities for a given ground excitation (green arrow). If an elastic layer is inserted, the corresponding floor velocity attenuation represents then the vibration attenuation perceived by the inhabitants (usually measured at floor mid span according to ISO standards [5]). The configuration with isolator also allows estimating the isolator upstream and downstream velocities in order to check the performance as indicated in section 2.3.
- the ground-foundations configuration in Figure 3b allows estimating the source free velocity (velocities on top of the foundations) as well as the source mobility Y_S (ratio velocity/force when a force is applied on top of the foundation).
- the disconnected building upper-structure in Figure 3b allows estimating the receiver mobility Y_R (ratio velocity/force when a force is applied at the foot of the upper-structure).

In this (rather far apart) two contact point source receiver system, the source and receiver transfer mobilities are supposed to be small compared to the source and receiver input mobilities respectively, so that each contact point can be studied independently and characterized by the source and receiver input mobilities only; this assumption is probably not correct at very low frequencies.

3.2 *FEM BEM approach*

The CSTB BEM-FEM ground structure vibration interaction model (MEFISSTO software, [6]) has been used. With the FEM (Finite Element Method) the entire domain considered is

meshed whereas with the BEM (Boundary Element Method) only the domain boundaries are meshed which in 2D leads to meshing simple contours. The basic configuration consists of a half space ground (BEM approach) and a building (FEM) with building elements either underground or above ground. Although the ground surface is of infinite extend, in practice only a limited portion of it is meshed beyond the area of interest; this is possible because of the strong absorption in the ground. Continuity of displacement and stress is assumed at common boundaries between domains.

FEM and BEM calculations are performed in narrow frequency bands, but all the frequency spectra given in this paper are expressed in a more robust way in 1/3 octave bands and obtained by energy summation of the narrow band results within each 1/3 octave band for velocities, and by applying the following equation for mobility magnitudes:

$$\left|Y_{1/3oct}\right|^2 = (1/N)\sum_{i=1}^{N}\left|Y_i\right|^2 \qquad (14)$$

(assuming N narrow bands in the 1/3 octave band considered).

3.3 *Geometry and material characteristics*

Details of the geometry of the ground-building configuration studied are given in Figures 4a and b; nine node FEM elements and two node linear BEM elements have been used.

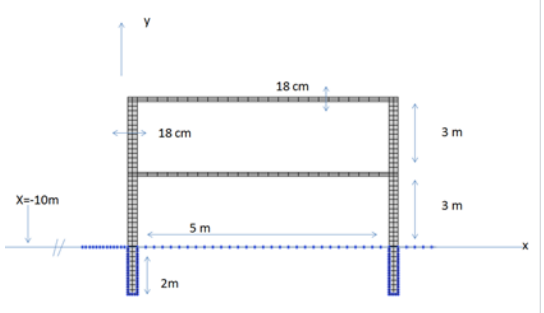

Figure 4a. Ground building configuration: geometry

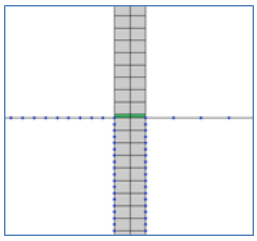

Figure 4b. Elastic layer: details; thickness: 6cm

The material characteristics associated with the half space homogeneous ground, the concrete structures and the elastic layer are given in Table 1.

Table 1. Material characteristics

	Young modulus	Loss factor	density	Poisson ratio
ground	270 MPa	0.10	1500 kg/m^3	0.26
structures	28 GPa	0.01	2400 kg/m^3	0.15
Elastic layer	6 MPa	0.10	1100 kg/m^3	0.26

The elastic layer dynamic stiffness K has been chosen as follows:

$$K = E.S/e \qquad (15)$$

where E is the Young modulus given in Table 1, S the layer surface area (0.18 x1 m^2 in the 2D geometry chosen) and e its thickness (6cm), which leads to K=18000 kN/m per meter length for each contact point. The weight of the upper-structure is close to M=4750 kg per meter length for each contact point, which leads to the following resonance frequency (assuming the upper-structure a lump mass):

$$f_r = (1/2\pi).\sqrt{K/M} \approx 10Hz \qquad (16)$$

3.4 *Dominant wave type*

Using the model, the power transmitted to the upper-structure can be estimated directly from stress and velocity at the contact points, and be separated into longitudinal (vertical) and bending wave powers. The longitudinal and bending wave powers transmitted without elastic layer to the upper-structure with a excitation force of 1N/m applied to the ground surface at 10 m from the building are compared in Figure 5.

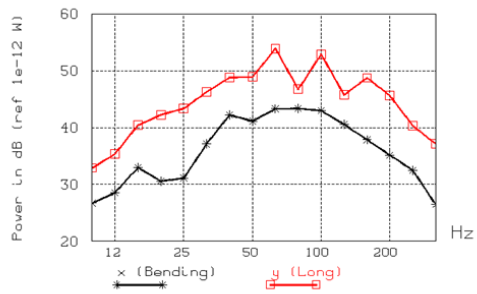

Figure 5. Power transmitted to the upper-structure (no isolator) in 1/3 octave bands (dB ref. 10^{-12} Watt); longitudinal waves (red curve), bending waves (black curve)

The longitudinal wave power is dominant (about 10 dB higher), which allows using the estimations developed in section 2 applied to longitudinal waves. All the PFIG results given below have been obtained by applying the equations of sections 2.2 and 2.3 to the (dominant) longitudinal (vertical) waves at the contact points.

3.5 *Floor vibration attenuation*

As explained in section 3.1, the floor velocity can be estimated with and without isolator using the 2D model

applied to the configuration given in Figure 3a, thus leading to the vibration attenuation perceived by the inhabitants. Figure 6 shows the two floor velocity levels at mid span before and after mitigation and Figure 7 shows the corresponding attenuation (negative insertion gain).

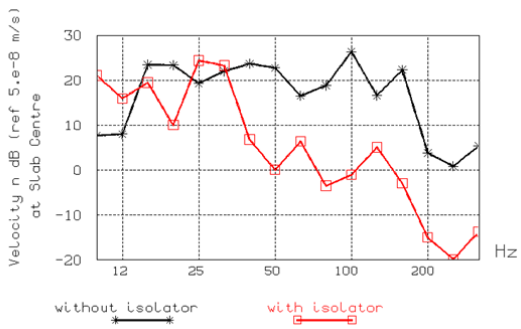

Figure 6. Floor velocity levels at mid span before and after mitigation

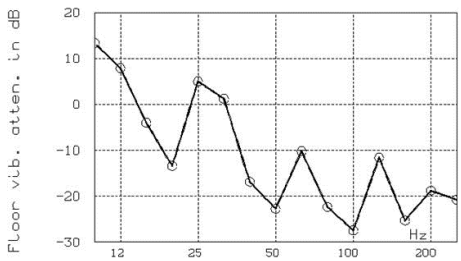

Figure 7. Floor velocity attenuation (negative insertion gain) at mid span in 1/3 octave bands

The results show a strong modal response of the isolated upper-structure between 25 and 31.5 Hz.

3.6 *Reference PFIG*

A reference PFIG can be determined from the (usually unknown) contact velocity v_c (without isolator) and the upstream velocity v_r (with isolator) using equation (12). This reference PFIG is given in Figure 8 for the two contact points; similar results are obtained. The results show that a significant insertion gain (-6 dB) is obtained from 1/3 octave 31.5 Hz. The isolator resonance at 12 Hz is clearly seen.

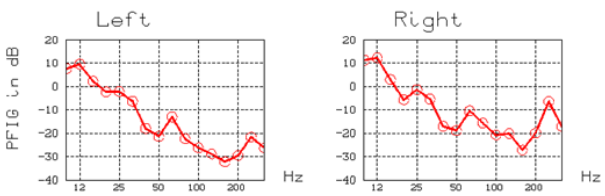

Figure 8. Reference PFIG determined from equation (12) for the two contact points (left and right) in 1/3 octave bands

3.7 *Predicted PFIG*

The PFIG estimate developed in section 2.2 allows predicting the isolator performance from the mobility of the source Y_S (foundations), the receiver Y_R (upper-structure) and the elastic layer Y_d. Y_S and Y_R have been numerically calculated using the model and Y_d has been determined either using the model or from the dynamic stiffness K of the elastic layer as:

$$Y_d = j\omega / K \tag{17}$$

The magnitudes of all the mobilities required are given in 1/3 octave bands in Figure 9.

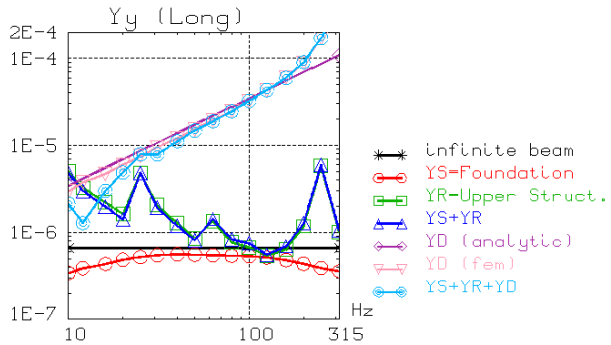

Figure 9. 1/3 octave mobility magnitudes used to predict the PFIG of the elastic layer

The resulting PFIG calculated from equation (9) is given in Figure 10.

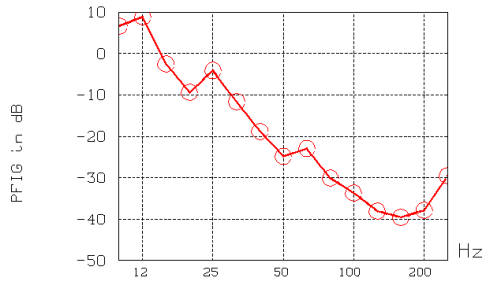

Figure 10. PFIG predicted from equation (9) in 1/3 octave bands

3.8 *"On site" PFIG*

The model allows estimating the isolator upstream and downstream velocities in order to check its performance as indicated in section 2.3. Equation (13) is then calculated from the velocities and mobilities determined by the model, leading to the PFIG shown in Figure 11 for the two contact points; similar results are obtained, except at the resonance frequency.

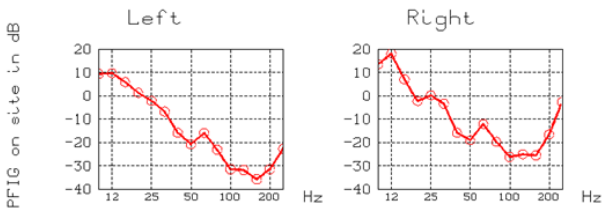

Figure 11. "On site" PFIG determined from isolator upstream and downstream velocities (equation (13)) in 1/3 octave bands

3.9 Comparison between the different PFIG estimates

The predicted PFIG (from section 3.7) and the "on site" PFIG (from section 3.8) are compared to the reference PFIG (from section 3.6), as well as to the well-known dynamic transmissibility of the "equivalent" single degree of freedom mass-spring oscillator; the results are given in Figure 12 in the case of the left contact point.

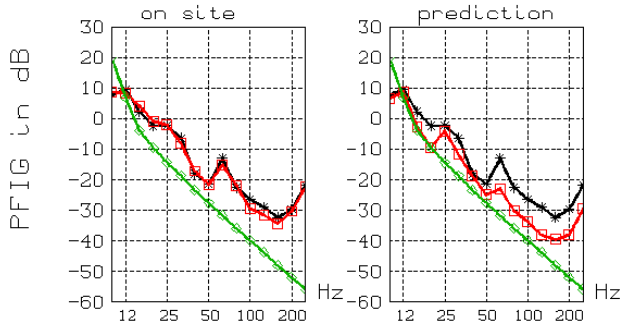

Figure 12. Comparison between the PFIG estimates (in red) and the reference PFIG (in black); the transmissibility of the mass-spring oscillator (in green) is also given .

The results show that (i) the transmissibility of the equivalent mass-spring oscillator really overestimates (of about 10 dB) the performance of the isolator, (ii) the "on site" PFIG, determined from measurements of the isolator upstream and downstream velocities is a very good estimate, (iii) the predicted PFIG overestimates the isolator performance, slightly at low frequencies, and more in the upper frequency range; nevertheless, this prediction is better than using the transmissibility of the equivalent mass-spring oscillator.

3.10 PFIG and floor velocity attenuation

The reference PFIG (from section 3.6) is now compared to the floor velocity attenuation at mid span (from section 3.5); the results are given in Figure 13, showing that the (calculated) modal response of the floor is rather rough and oscillates around the reference PFIG.

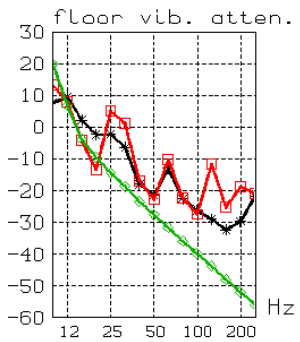

Figure 13. Comparison between the reference PFIG in dB (in black) and the floor velocity attenuation at mid span (in red); the transmissibility of the mass-spring oscillator (in green) is also given

3.11 Useful approximations

In the equations estimating the predicted and "on site" PFIG, respectively (9) and (13), the mobility terms are difficult to estimate because they are complex quantities. Expressions using only mobility magnitudes would be easier to estimate (by measurement or calculation).

Figure 9 shows that the magnitude of Y_S+Y_R is close to the sum of the magnitudes of Y_S and Y_R, thus leading to the following approximation for the "on site" PFIG:

$$PFIG \approx 10.\lg\left(\frac{v^2_{r,rms}}{v'^2_{c,rms}}.(|Y_R|^2+|Y_S|^2)/|Y_R|^2\right) \qquad (18)$$

Figure 9 also shows that the same approximation can be applied to the magnitude of $Y_S+Y_R+Y_d$ but only above 20 Hz:

$$\begin{aligned} PFIG &\approx 10.\lg((|Y_S|^2+|Y_R|^2)/(|Y_S|^2+|Y_R|^2+|Y_d|^2)) \\ &\approx 10.\lg((|Y_S|^2+|Y_R|^2)/|Y_d|^2) \end{aligned} \qquad (19)$$

At 20 Hz and below, around the isolator resonance frequency, complex mobilities shall be used to correctly estimate equation (9) and consequently equation (19) is not valid; Figure 14 compares these two equations and clearly shows the limits of the approximation.

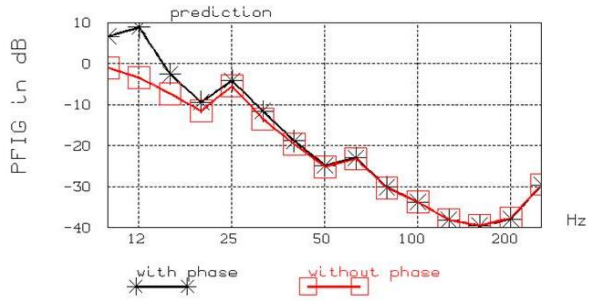

Figure 14. Comparison between the PFIG predicted from equation (9) (in black) and the approximation using equation (19) (in red)

4 CONCLUSION

In this paper a method for predicting and checking on site the performance of isolators inserted in buildings for protection against environmental vibration has been proposed. The prediction requires the knowledge of the longitudinal (vertical) input mobility of the building foundations, the building upper-structure and the isolator; the method overestimates a little the performance. Measuring on site the isolator upstream and downstream velocities leads to another estimate of the isolator performance, more precise than the prediction. The results also show that the well-known dynamic transmissibility of the equivalent one degree of freedom oscillator overestimates the isolator performance. The method was numerically validated using a 2D FEM BEM ground building model, which showed the limits of the method, particularly if only mobility magnitudes are used in the prediction. The use of this simple method is only possible if the power is transmitted to the receiver through a dominant wave type and if the contact points or lines between source and receiver are far apart (uncorrelated) and can therefore be treated separately.

ACKNOWLEDGMENTS

The authors gratefully acknowledge the financial support of this study by the French Agency ADEME (Agency for Environment and Energy Management).

REFERENCES

[1] Talbot J.P. and Hunt H.E.M., "On the performance of base-isolated building", Building Acoustics, Vol.7, n°3 (2000), pp. 163-178
[2] M. Ohlrich, "Structure borne sound sources and their power transfer", Inter-noise 2001, The Hague, The Netherland, Proceedings
[3] ISO 7626 series, Vibration and Shock – Experimental determination of mechanical mobility
[4] Mayr A.R. and Gibbs B.M., "Single equivalent approximation for multiple contact structure-borne sound sources in buildings", Acta Acustica 98 (2012), 402-410
[5] ISO 2631-2, Mechanical vibration and shock – Evaluation of human exposure to whole-body vibration –Part 2: Vibration in buildings (1 Hz to 80 Hz)
[6] Jean P., "Boundary and finite elements for 2D soil-structure interaction problems", Acta Acustica 87, 2001, 56-66